

Accurate Aerial Image Simulation Using High-Resolution Reticle Inspection Images

William B. Howard*, Chris A. Mack

KLA-Tencor, 8834 North Capital of Texas Highway, Suite 301, Austin, Texas 78759, USA

ABSTRACT

The use of hardware-based and software-based reticle defect printability simulation systems is expanding as the cost and complexity of reticles increases. Without such systems it has become increasingly difficult to predict the lithographic significance of a defect found on a reticle. The viability of such systems can be judged using several criteria including accuracy, ease of use, level of automation, and the degree to which they can be applied to a wide range of reticle types. Simulation systems have improved in each of these areas. Automated and semi-automated systems have now been developed and integrated into reticle manufacturing. We report on advances made in a software-based simulation system which uses high-resolution reticle inspection images as the basis for the description of the reticle. We show that the simulated aerial images can be compared quantitatively to results from a hardware-based simulation system (the Zeiss AIMS™ tool) for both 193 and 248 nm EPSM reticles. The development of a new set of metrics to judge lithographic significance will be explained. Common procedural mistakes in evaluating the impact of a defect will be discussed.

Keywords: defect printability, PROLITH, AMDD, simulation

1. INTRODUCTION

1.1. Reticle Defect Printability and Disposition

As k1 factors have declined and RET solutions have become more complex, the ability to accurately determine the lithographic significance of reticle defects using visual techniques and size-based metrics alone has diminished. As one example, operators cannot be expected to estimate the local mask error enhancement factor (MEEF) value with any degree of accuracy and then add this consideration to the defect disposition. The situation is further complicated by the variability of human judgment. Different operators will disagree on defect sizes and relative importance and even the same operator might change their mind with increased experience. When disputes arise, the lack of precise and reproducible metrics hinders resolution.

The most common result is that reticle manufacturers adopt a conservative approach but retain the defect size paradigm. A defect size specification that is excessively conservative leads to lengthened cycle time, unneeded repairs, and increased costs. The unneeded repairs, in turn, increase reticle handling and the possibility of damage. Also, some defects that are erroneously judged as important might not be repairable and the reticle might be scrapped unnecessarily.

Even with the most conservative approach, simple mistakes can occur in the defect disposition process and printable defects can be misclassified as insignificant. Although these events are rare, the impact can be devastating in terms of cost, cycle time, and the level of trust between reticle suppliers and reticle users. It is desirable to have an independent verification for 100% of the disposition results.

What is needed, then, is a way to accurately disposition reticle defects based on lithographic science. The method must be accurate, practical, reproducible, and objective. The value of such an approach would be optimized if it could also quickly verify the current disposition of all defects and be automated.

*William.Howard@KLA-Tencor.com; phone 512-231-4249; fax 512-346-9542

In this paper we report on advances made in a software-based simulation system for reticle defect disposition. This system uses high-resolution reticle inspection images as the basis for the description of the reticle. The method is grounded in lithographic science and has been designed for the characteristics mentioned above.

1.2. Methods for Determining Lithographic Impact

There are multiple ways to disposition reticle defects based on their lithographic impact. The most common method for the initial disposition remains the use of defect size. However, as has been mentioned, this criterion alone does not accurately or efficiently take into account important factors such as optical proximity and illumination configuration. However, size is a useful criterion to collect defects into large bins for further analysis. The largest defects are likely to be problematic regardless of the wafer process used and these are routinely repaired.

Wafer print studies could be done to determine the correct defect disposition. However, this process is impractical in most cases, especially as an initial disposition method, because it is expensive and because the equipment needed for such an evaluation is not typically at the reticle manufacturing centers. One can imagine how difficult it would be for a commercial reticle manufacturer to replicate the wafer process of multiple customers.

A third method is to use lithography simulation. Lithography simulation is used to predict the lithographic impact of the defect by simulating the aerial image or resist image that would result from the reticle. These methods are based on lithographic science and avoid the obvious difficulties of printing wafers for every reticle at multiple inspection points. There are two general classes of lithography simulation for reticle defects—hardware simulation and software simulation.

Hardware simulation uses an optical system to emulate the illumination system and generate an aerial image that approximates that of the true stepper. The AIMS™ systems from Zeiss are a good example of such systems and they are in wide use in the industry.

Software simulation uses lithographic models to predict the impact of defects. To clarify how such a system works, we consider the specific solution used for this research. First, a general overview of the process will be given, and then some details of important steps will be examined.

2. AMDD

2.1. AMDD Overview

A prototype of the automated mask defect disposition system (AMDD) was used to study the accuracy of software simulation by comparing the results to hardware simulation. Figure 1 shows the most important steps of the process.

The first step is the inspection of the reticle using the KLA-Tencor F-series or TeraScan systems. This results in the acquisition and storage of image pairs for each of the reticle defects. The two images represent the defective area of the reticle (called the “test” image) and the non-defective area (called the “reference” image). The pair of images is referred to as a test and reference image pair or TRIP. The reference image is either a captured image of a non-defective die in the case of Die-to-Die (DD) inspection or a rendered database image in the case of Die-to-DataBase (DDB) inspection. The inspection images are stored in a multi-page TIFF file. A text file provides information to link the images to the defect list. At the completion of the inspection process, each TRIP is converted to simulation masks in a format used by PROLITH™ simulation software. A PROLITH template file that has been configured to match the stepper conditions is then accessed and separate aerial image simulations are conducted for the test and reference. A metric extraction algorithm then generates a series of 1D and 2D metrics to be used to disposition the defects. To complete the disposition process, a series of disposition criteria are used to compare the metrics to various limits. The final result for each defect is the complete set of metrics and a disposition result which is “pass”, “fail” or “warn.”

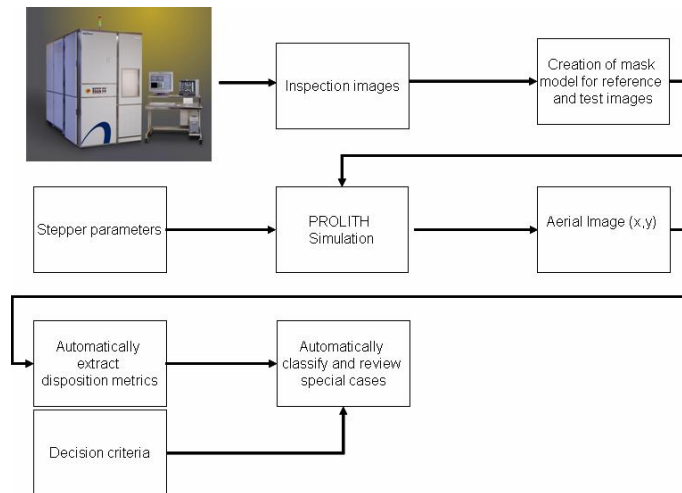


Figure 1: Flow diagram of AMDD. Following reticle inspection, each TRIP is converted to two simulation masks. Then, parallel simulations are conducted for the test and reference. The differences between the two simulations are quantified when metric extraction and disposition completes the process.

2.2. Aerial Image and Resist Profile Simulation

The stepper parameters needed for the simulation are: illumination wavelength, source shape and numerical aperture (NA). The optional specification of aberrations is supported. The source shape can be measured, parametrically defined or specified via input file for source shapes not covered by the parametric definitions.

Resist profile simulation is also supported using the PROLITH full physical model (FPM) or lumped parameter model (LPM). The first of these resist models is the most accurate on an absolute basis. However, the LPM is much faster and, for reticle defect printability where differential accuracy (i.e., the difference between the test and reference simulations) is most important, it is generally a better choice.

Finally, all the simulations can be run through stepper focus and exposure variation to determine if the defect reduces the process window or to evaluate the worse case printability of the defect. In this study, the defects were simulated only through the aerial image stage and only at nominal focus and exposure.

2.3. Metric Extraction and Disposition

AMDD uses two classes of metrics to disposition reticle defects. The first class of metrics is based on image intensity difference and is applicable only to aerial image simulation. The second class of metrics is based on shapes of either the aerial image intensity contours or the resist profile. Both classes of metrics are explained below although only the intensity difference metrics were used in this study.

2.3.1. Intensity Difference Metric

Consultations with various AIMS users have shown that most of them use intensity metrics to judge the printability of reticle defects. To study how the defect has changed the intensity profile, operators typically use a 1-D metrology plane that intersects the defect. Further, it is common to use a standard of 10% for determining whether a defect should or should not be repaired. That is, if the intensity metric is less than 10%, the defect is not repaired. As part of this study, we used such a metric to better understand and quantify the printability issue. The 1D-intensity difference metric (1D-IDM) is defined by Equation 1:

$$1D - IDM = 100\% \times \frac{|I_{Ref} - I_{Test}|}{MaxRange} \quad (1)$$

The values in the numerator are taken at the location along the 1D metrology plane where the test and reference aerial images differ by the largest amount. Using the absolute value ensures that the 1D-IDM is always a positive number expressed as a percent. The denominator is the normalization factor, which is calculated from the maximum range of the aerial images along the 1D metrology plane in the vicinity of the defect location. Figures 2a and 2b show two examples to illustrate how the IDM is defined.

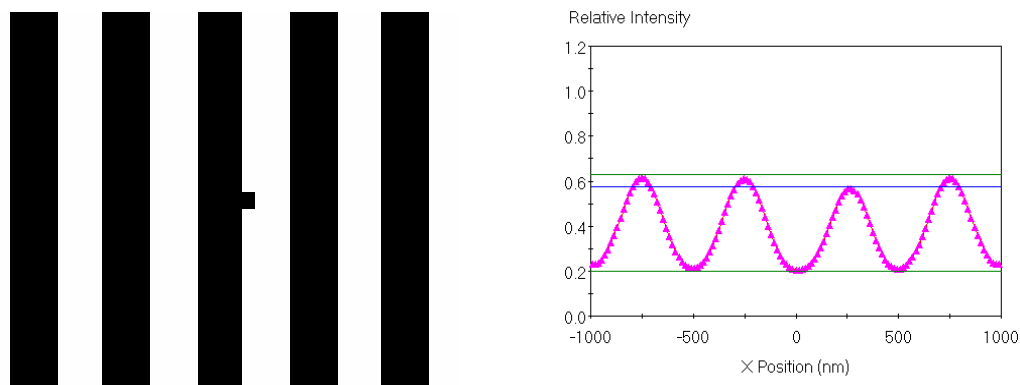


Figure 2a: A simulation mask with chrome extension (left) and the resulting aerial image intensity along a horizontal metrology plane centered on the defect (right). The nominal peak and trough intensities of the aerial images are shown with dashed horizontal lines and the drop in intensity of the peak is shown with a solid line.
 $1D-IDM = 100\% \times |.62-.58|/(.62-.20) = 9.5\%$.

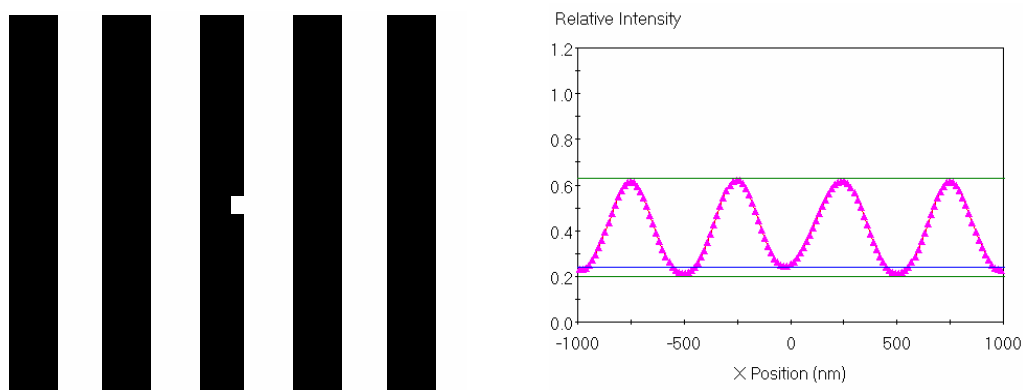


Figure 2b: A simulation mask with quartz extension (left) and the resulting aerial image intensity along a horizontal metrology plane centered on the defect (right). The nominal peak and trough intensities of the aerial images are shown with dashed horizontal lines and the increase in intensity of the trough is shown with a solid line.
 $1D-IDM = 100\% \times |.25-.20|/(.62-.20) = 11.9\%$.

Our research has shown that use of this 1D-IDM metric can be problematic. These problems will be discussed in Section 4 below. To address these problems, we have created a new two-dimensional IDM (2D-IDM) that is better suited for defect disposition. A comparison of Equation 2 to Equation 1 shows that the forms of the two metrics are identical. Only the method of calculation is different. To calculate the 2D-IDM, AMDD automatically determines the location, $P_{max}(x,y)$, of the greatest aerial image difference between the test and reference. The intensity difference at this point is the numerator in Equation 2. The denominator in Equation 2 is generated by a proprietary algorithm. A simplified version of this process is depicted in Figure 3.

$$2D-IDM = 100\% \times \frac{|I_{Ref} - I_{Test}|}{NormalizationFactor} \quad (2)$$

The algorithms that were used to calculate the 2D-IDM from the AMDD simulations can also be used to calculate 2D-IDM values from exported AIMS files.

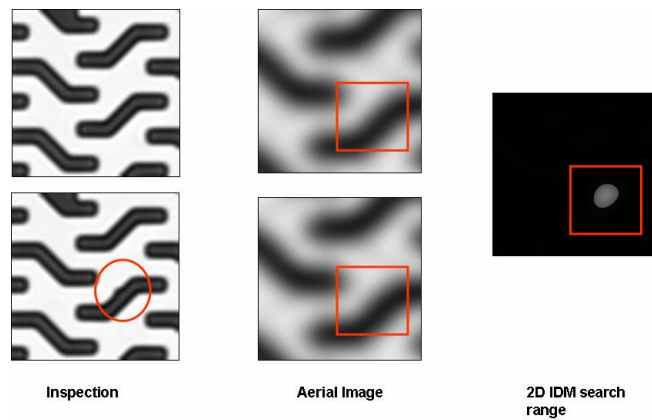


Figure 3: A simplification of the process used to generate the 2D-IDM. The reference (top) and test (bottom) inspection images are used to create simulation masks and then the aerial images. An algorithm determines the point of interest $P_{\max}(x,y)$ and the intensity difference at this point is calculated. A second algorithm calculates the normalization factor.

2.3.2. Shape-Based Metrics

The second class of metrics in AMDD uses shape-based algorithms. These metrics are generated from the shapes of the aerial image intensity or resist image contours. In the case of aerial image contours, a preliminary CD calibration step is used to determine the aerial image threshold (contour intensity value) that will yield the correct wafer resist image CD. This calibration procedure is done only once for each inspection. The contour shapes (aerial image or resist image) represent each feature on the printed wafer. These contours are extracted for the test and reference and then compared to each other. A series of metrics can then be extracted which include: area difference, overlapping area, maximum edge placement error (MEPE), etc. Figure 4 shows a depiction of the MEPE metric.

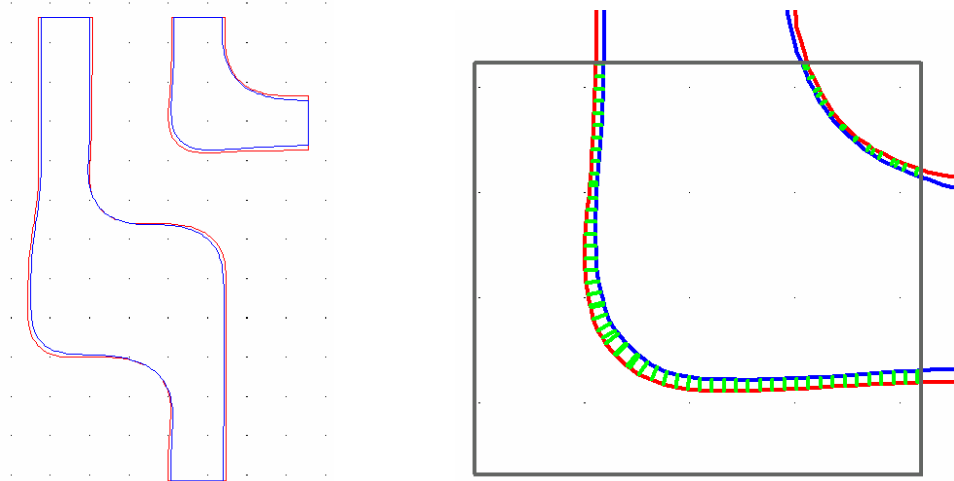


Figure 4: The MEPE. The resist image profile of the reference (red) is compared to that of the test (blue). Along the perimeter, a set of vectors (green) are used to represent the edge displacement. The length of a single vector is the Edge Placement Error (EPE) at that point. The largest EPE for the simulation region is the MEPE.

2.4. Automation

As mentioned above, any manual system is prone to operator error, operator variability and simple mistakes. The ideal solution would be able to check the existing defect disposition. AMDD is especially well suited for this task as it can process defects at a high rate and check to ensure that no gross errors occurred. The entire process shown in Figure 1 can be automated.

3. REVIEW OF PREVIOUS RESULTS

A system similar to AMDD called PRIMADONNA has been used in a production environment since 2002¹. During one published study, PRIMADONNA was used in parallel with hardware simulation to quantify various metrics of usability and accuracy. Most importantly, this system was found to generate no “fatal mistakes”. That is, PRIMADONNA did not disposition any defects as “passed” which were classified by AIMS as “failed”. Additionally, it was estimated that the number of defects requiring labor-intensive disposition could decrease by 35% and the total number of captured defects requiring repair could decrease by 45%².

A second study was conducted to evaluate a wider range of defect disposition techniques and to compare the results of AMDD to both AIMS and wafer print results³. A programmed 193nm technology EPSM defect reticle was used and inspected with a TeraScan system. Figure 5 shows a comparison of AMDD and AIMS based on the change in CD caused by 82 of the programmed defects. The correlation, linearity and offset are good. Comparison of AMDD and AIMS for a single defect type is shown in Figure 6. Again, the correlation is good.

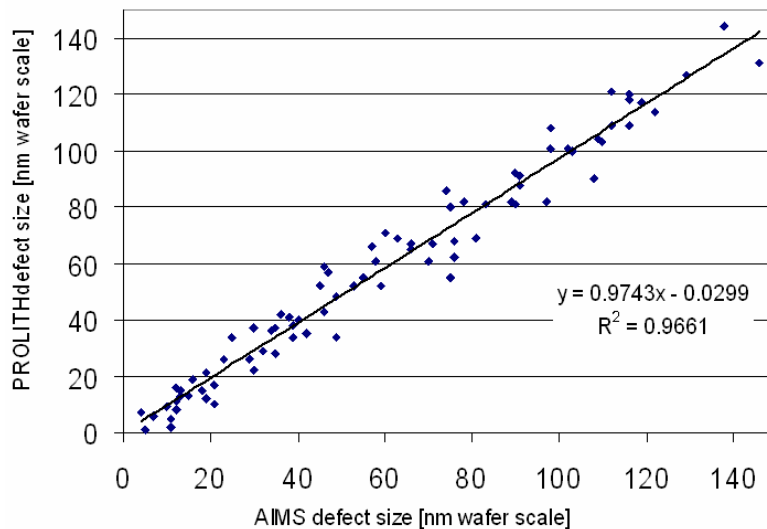


Figure 5: Comparison of change in CD for AMDD (PROLITH) and AIMS simulations. A 193nm technology EMPS programmed defect reticle was used.

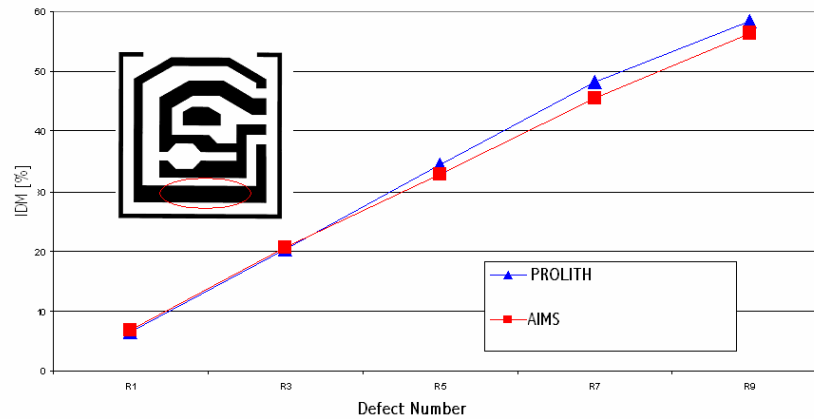


Figure 6: Comparison of 2D-IDM for AMDD (PROLITH) and AIMS simulations. A single defect type from the reticle is represented. In this case, the defect consisted of a horizontal line that was made progressively wider.

4. PURPOSE, RESULTS AND DISCUSSION

4.1. Purpose

The first purpose was to compare the results from AMDD to those from hardware-based simulation and quantify the degree to which the two systems match. For this comparison, the 2D-IDM metric was used. The second purpose of this research was to develop and test improvements to AMDD to enhance accuracy and efficiency.

4.2. Test Reticles

For this study, we used two programmed Spica defect reticles that were inspected on a KLA-Tencor TeraScan system. Both reticles were EPSM versions—one for 193nm technology and one for 248nm technology. For each inspection, we selected a sampling of defect sizes from each of the 14 defect types. To provide a good sampling of defects, we used every other defect size over a range of interest. The total number of defects analyzed was 166 (100 from the 193nm reticle and 66 from the 248nm reticle).

4.3. AMDD Results Compared to AIMS

2D-IDM data was generated by AMDD as described in Section 2. To make a comparison to AIMS as accurate as possible, the AIMS simulation data were also processed through the same 2D-IDM algorithms. In the case of AIMS simulations, the test and reference aerial image simulations were not aligned automatically, so algorithms were created to accomplish this task prior to extracting the 2D-IDM values.

The results of the comparison are shown in Figures 7 and 8 for the 248nm and 193nm technology EPSM versions of the Spica, respectively. The illumination conditions are shown in the figures. The RMS value of the difference between AMDD and AIMS was 2.9% for both cases. It is important to note that the model is the same in both the 248nm and 193 nm cases—only the physically measurable parameters have changed. The confirmation that one model could work for both 248nm and 193nm EPSM was one measure of success. The correlation between the two methods shows good agreement and linearity with an offset of less than 2nm.

Spica 248 EPSM - - PROLITH to AIMS Correlation

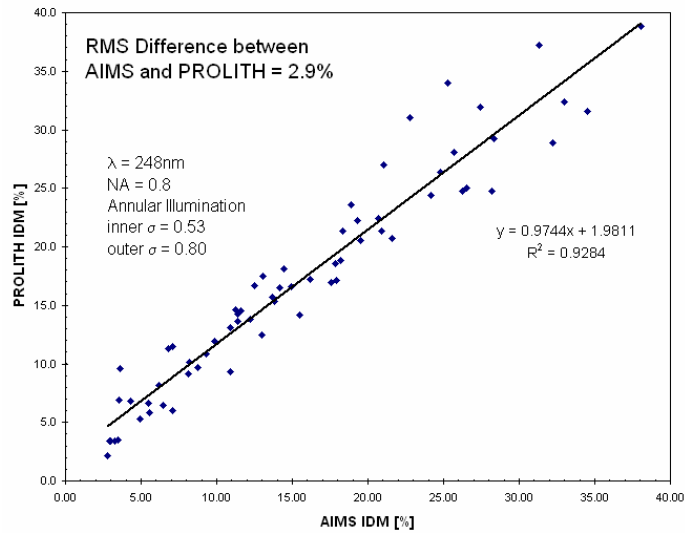


Figure 7: Comparison of 2D-IDM for AMDD (PROLITH) and AIMS simulations for the 248nm technology EPSM Spica reticle.

Spica 193 EPSM - PROLITH to AIMS Correlation

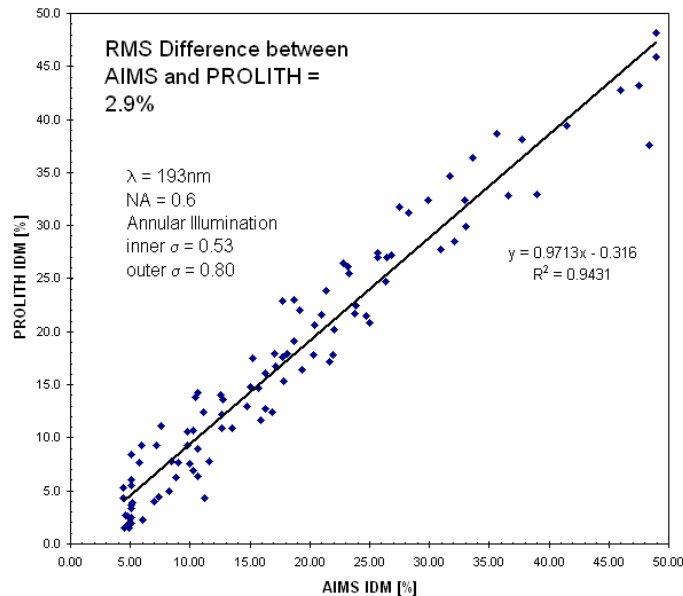


Figure 8: Comparison of 2D-IDM for AMDD (PROLITH) and AIMS simulations for the 193nm technology EPSM Spica reticle.

4.4. Algorithm Improvements

4.4.1. Creation of Simulation Masks

To achieve accurate results, one of the most important steps in the AMDD process is the conversion of the F-series or TeraScan inspection images to PROLITH simulation masks. The conversion uses a proprietary algorithm that has two important characteristics. First, it was developed by modeling the image acquisition system of the F-series and TeraScan configurations. Second, the parameters for the conversion algorithm are limited to physically meaningful and measurable parameters. These include the actual phase and transmission of the background (chrome or EPSM) and the

light calibration values from the inspection. The conversion process is not applicable to reticles with more than two tones or two phases. This conversion process was used for the results presented here as well as those shown in Figures 5 and 6.

4.4.2. Improvements to IDM

The aerial image is, fundamentally, a 2D quantity. To use the 1D-IDM, the user must select a metrology plane that effectively reduces the 2D aerial image into a set of 1D images. As was mentioned in Section 2, we found this approach problematic and, therefore, we created the 2D-IDM. Here we discuss the various problems we encountered with the 1D-IDM.

We have witnessed multiple problems with the selection of the appropriate 1D metrology plane for analysis. In simple cases where the reticle pattern is a series of dense lines oriented in the x or y direction, the selection of the appropriate plane is not difficult. For example, if the lines are vertical, the user creates a horizontal metrology plane which can be moved perpendicularly to find the greatest intensity change as shown in Figures 2a and 2b. However, this process is very complicated for defects on corners or non-arrayed patterns and we have observed operator errors in these cases. In particular, the choice of metrology planes is subjective and not reproducible. Again, this is especially so when the geometry is not regular.

The second problem of appropriate normalization can be best explained through an example. Figure 9 shows the aerial image intensity across a 1D metrology plane. The pattern in this case is not complicated – a simple dense line/space pattern. The defect occurs where the peak intensity drops and is depicted as a circle. To generate the 1D-IDM, one must select a non-defective peak and trough as the reference. However, different operators will pick different peaks as the reference resulting in different 1D-IDM values. For this example, the range of 1D-IDM values is 14% +/- 4% depending on which normalization is used.

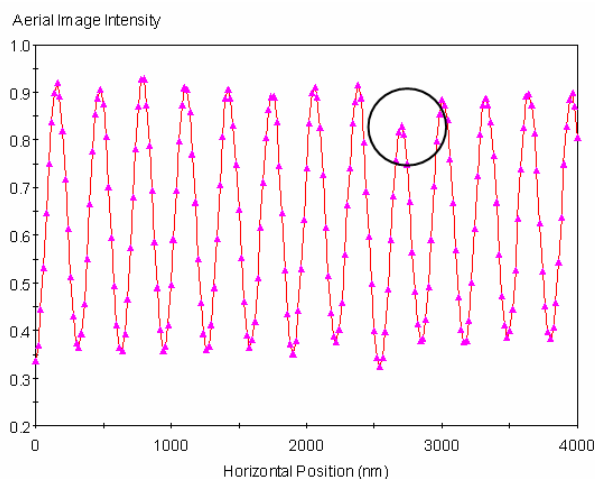


Figure 9: Aerial image intensity along a 1D metrology plane taken from an AIMS file. In this case, the peak and trough intensities vary across the metrology plane and the calculated IDM will and the denominator in the 1D-IDM will vary as well. The variation of the peak and trough intensities could be the result of varying OPC across the pattern, variation in the reticle process, presence of a large “stain” defect, or some other cause. Regardless, operators might choose any of these adjacent peaks for normalization and arrive at a different 1D-IDM value.

The problems with the 1D-IDM are not limited to AIMS systems, and occur when using PROLITH aerial images as well. The issue is one of procedure, not equipment. Figure 10 shows another example of this problem, this time using PROLITH images. Two different defect types were first analyzed manually by setting 1D metrology planes. Then they were analyzed automatically through the use of our 2D-IDM algorithms. In one case (defect type E), the results were significantly different. In the second case (defect type H), they were mostly similar.

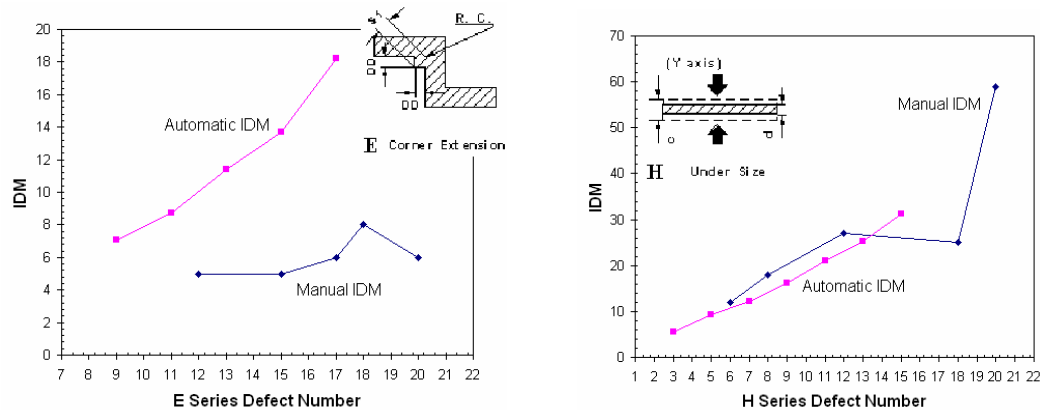


Figure 10: Comparison of manual 1D and automatic 2D method of calculating IDM using PROLITH aerial images. Defect type E is a corner defect and the location of the appropriate metrology plane is more problematic. Defect type H is a thinning line in a regular horizontal brick pattern and the appropriate metrology plane is more obvious.

5. CONCLUSIONS

The work presented here has confirmed the results of earlier studies. AMDD gives results that are consistent with AIMS results for both CD and IDM metrics. The two systems can work together in a way that utilizes the relative advantages of both. AMDD is well suited for the additional task of validating the current disposition of all defects by quickly checking for any gross errors.

Well-designed metrics are essential to achieving reproducible and accurate results. Automating the metrics greatly improves the reproducibility and makes the determination of IDM equally easy for any pattern type. To correctly compare software and hardware simulation results, the same metrics and algorithms should be used.

The agreement between AMDD and AIMS was similar for both of our 248nm and 193nm EPSM test cases with an RMS value of 2.9% for both. These data suggest that the algorithm to convert inspection images to simulation masks is effective. Restricting the conversion parameters to values that are physically meaningful and measurable has greatly improved the usability of the algorithm.

6. FUTURE WORK

We plan to extend our work to cover a wider range of reticles covering more design layers and technology nodes. Additionally, we will be expanding our research to include resist modeling, starting with the LPM model. We have also identified some algorithm changes for metric extraction.

ACKNOWLEDGMENTS

The authors would like to thank the staff of Photonics for assistance in gathering the AIMS data.

REFERENCES

1. D. Bald, S. Munir, B. Lieberman, W. Howard, C. Mack, "PRIMADONNA: A System for Automated Defect Disposition of Production Masks Using Wafer Lithography Simulation," in *22nd Annual BACUS Symposium on Photomask Technology*, B. Grenon, K. Kimmel, Editors, Proceedings of SPIE Vol. 4889, pp. 263-270, (2002).
2. S. Munir, D. Bald, V. Tolani, F. Ghadiali, "DIVAS: An Integrated Networked System for Mask Defect Dispositioning and Defect Management," in *Cost and Performance in Integrated Circuit Creation*, A. Wong, K. Monahan, Editors, Proceedings of SPIE Vol. 5043, pp. 114-122, (2003).
3. A. Nhiev, J. Hickethier, H. Zhou, T. Hutchinson, W. Howard, M. Ahmadian, "A Study of Defect Measurement Techniques and Corresponding Effects on the Lithographic Process for a 193nm EPSM Photomask," in *23rd Annual BACUS Symposium on Photomask Technology*, K. Kimmel, W. Staud Editors, Proceedings of SPIE Vol. 5256, pp. 1120-1129, (2003).